https://doi.org/10.48196/021.01.2025.04

Submitted: *June 03, 2025*
Received in final revised form: *June 27, 2025*
Accepted: *June 29, 2025*

Development of a Spray Droplet Size Test Rig for Knapsack Sprayers

Philharks Allen N. Que[1], Arthur L. Fajardo[2], Ralph Kristoffer B. Gallegos[3], and Mark Angelo F. Ranches[4]

[1]BS Agricultural and Biosystems Engineering Graduate, Agribiosystems Machinery and Power Engineering Division (AMPED), Institute of Agricultural and Biosystems Engineering, College of Engineering and Agro-Industrial Technology, University of the Philippines Los Baños, College, Los Baños, 4031 Laguna, Philippines

[2]Professor 5, Agribiosystems Machinery and Power Engineering Division (AMPED), Institute of Agricultural and Biosystems Engineering, College of Engineering and Agro-Industrial Technology, University of the Philippines Los Baños, College, Los Baños, 4031 Laguna, Philippines

[3]Associate Professor 2, Agribiosystems Machinery and Power Engineering Division (AMPED), Institute of Agricultural and Biosystems Engineering, College of Engineering and Agro-Industrial Technology, University of the Philippines Los Baños, College, Los Baños, 4031 Laguna, Philippines

[4]Assistant Professor 1, Agribiosystems Machinery and Power Engineering Division (AMPED), Institute of Agricultural and Biosystems Engineering, College of Engineering and Agro-Industrial Technology, University of the Philippines Los Baños, College, Los Baños, 4031 Laguna, Philippines

Email: [1]philharksallen@gmail.com, [2]alfajardo@up.edu.ph (corresponding author), [3]rbgallegos@up.edu.ph, and [4]mfranches1@up.edu.ph

ABSTRACT

The determination of spray droplet sizes is an essential aspect of selecting spraying equipment. It influences the efficacy and safety of spraying operations. This study focuses on developing a spray droplet size test rig for agricultural sprayers. The design focuses on emulating the method of test for spray droplet measurement as per the Philippine National Standards (PNS/BAFS 332:2022). The rig consists of a linear positioning system with a carriage, timing belts, spray barriers, and a water-sensitive paper platform. A stepper motor and Arduino-based software were used for the control system. The highest coefficient of variation recorded in all trials was 1.09%. The analysis for the spray droplet sizes showed a low coefficient of variation of 5.91%. All of the tests yielded the same droplet size classification of "VERY COARSE". This is the same classification in the official test report. This indicates that the developed test rig can precisely determine spray droplet sizes. It is recommended to test the rig further using other types of sprayers.

Keywords: *sprayer, droplet size, test rig, precision, VMD*

INTRODUCTION

Sprayers are primarily utilized in agriculture for crop protection. Agrochemicals such as pesticides and herbicides are sprayed into target areas. The use of sprayers enables a safer and more cost-effective farm operation. There are various types of sprayers, including manual, animal-drawn, and power-operated sprayers. An example of a manual sprayer is a knapsack sprayer. Small to medium-scale farms benefit from them. The low initial and maintenance costs, along with ease of operation, make it highly accessible in terms of its operation (Anjum et al., 2023). These sprayers allow operators to walk around farm operations while spraying. This allows for controlled spraying on target areas (Bhuse, 2014).

Sprayer specifications influence droplet deposition in the target area. These include nozzle type and pressure settings, which affect the volumetric median diameter (VMD). Operational factors, such as motion speed and nozzle height, also impact VMD. As shown in **Figure 1**, a higher VMD leads to less adhesion on leaves. This increases the likelihood of agrochemicals reaching the soil. In contrast, a lower VMD improves droplet adhesion to leaf surfaces. Proper determination of VMD is important for selecting the appropriate agrochemical for a sprayer (ASABE, 2009).

Spray operations can also produce unwanted effects, such as spray drift. There is an inverse relationship between VMD and the potential for spray drift (Al Heidary et al., 2014). Farmers in the Philippines use pesticides for an average of 2.31 days per week. Very few farmers utilized protective equipment during the spraying operation (Lu, 2022). This reinforces the need for proper VMD determination.

The spray droplet sizes are measured using water-sensitive paper (WSP). The method of test involves six WSP sheets, each 20 mm × 30 mm, placed 150 mm apart. This setup simulates the spray swathe during actual operation as shown in **Figure 2**.

The target area should be cleared in approximately 1 second (BAFS, 2022). The speed and height of the nozzle influence spray distribution in the target area. The procedure is done manually by a test engineer, which may cause variations in height and spray times as well as speed of nozzle over the WSP. Inconsistent speed of nozzle over the WSP results to different VMD measurements. Test engineers run while trying to maintain a constant height for the sprayer. Another issue is the speed at which the test engineers run. AMTEC's test method has been changed to address this problem. Test engineers run while attempting to maintain a constant height. An additional issue is the speed at which the test engineers would run. The test method of AMTEC has changed to address this issue (**Figure 2**).

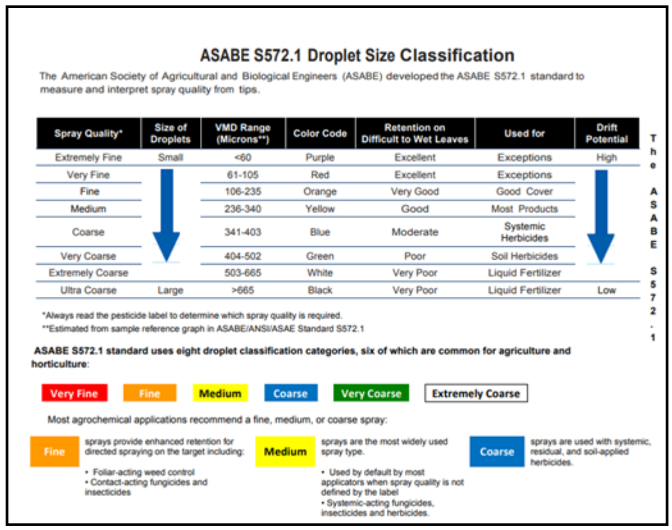
ASABE S572.1 Droplet Size Classification

The American Society of Agricultural and Biological Engineers (ASABE) developed the ASABE S572.1 standard to measure and interpret spray quality from tips.

Spray Quality*	Size of Droplets	VMD Range (Microns**)	Color Code	Retention on Difficult to Wet Leaves	Used for	Drift Potential
Extremely Fine	Small	<60	Purple	Excellent	Exceptions	High
Very Fine		61-105	Red	Excellent	Exceptions	
Fine		106-235	Orange	Very Good	Good Cover	
Medium		236-340	Yellow	Good	Most Products	
Coarse		341-403	Blue	Moderate	Systemic Herbicides	
Very Coarse		404-502	Green	Poor	Soil Herbicides	
Extremely Coarse		503-665	White	Very Poor	Liquid Fertilizer	
Ultra Coarse	Large	>665	Black	Very Poor	Liquid Fertilizer	Low

The ASABE S572.1

*Always read the pesticide label to determine which spray quality is required.

**Estimated from sample reference graph in ASABE/ANSI/ASAE Standard S572.1

ASABE S572.1 standard uses eight droplet classification categories, six of which are common for agriculture and horticulture:

Very Fine | Fine | Medium | Coarse | Very Coarse | Extremely Coarse

Most agrochemical applications recommend a fine, medium, or coarse spray:

Fine sprays provide enhanced retention for directed spraying on the target including:
- Foliar-acting weed control
- Contact-acting fungicides and insecticides

Medium sprays are the most widely used spray type.
- Used by default by most applicators when spray quality is not defined by the label
- Systemic-acting fungicides, insecticides and herbicides.

Coarse sprays are used with systemic, residual, and soil-applied herbicides.

Figure 1. Droplet size classification (Source: ASABE, 2009).

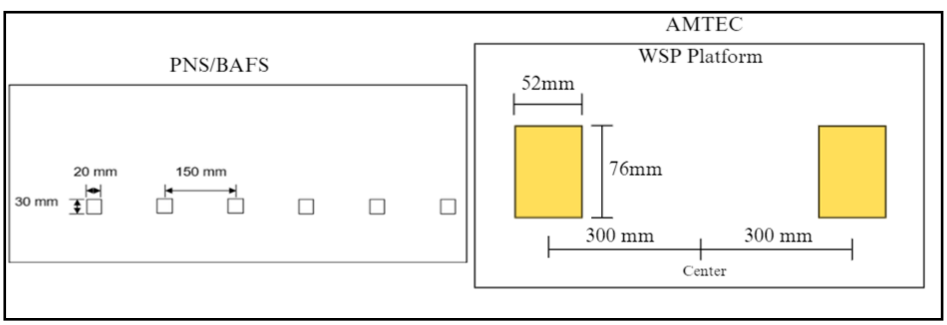

Figure 2. WSP card placement (PNS/BAFS, left; AMTEC-UPLB, right).

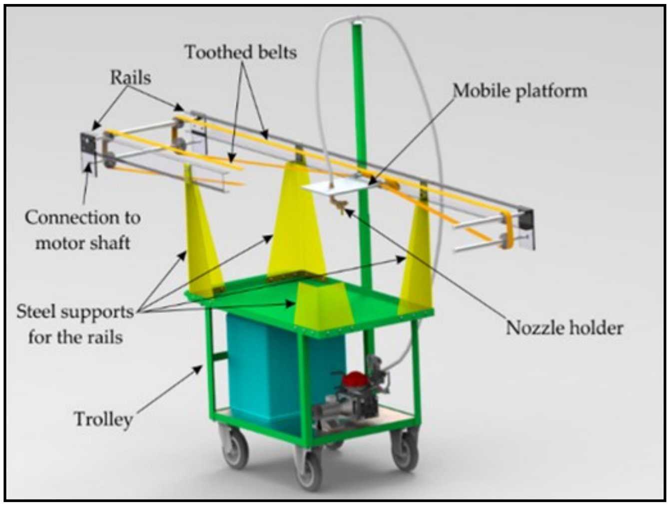

Figure 3. 3D model of test bench by *Longo D., et al., 2020*.

Figure 4. Spraying robot by *Jasim et al., 2023*.

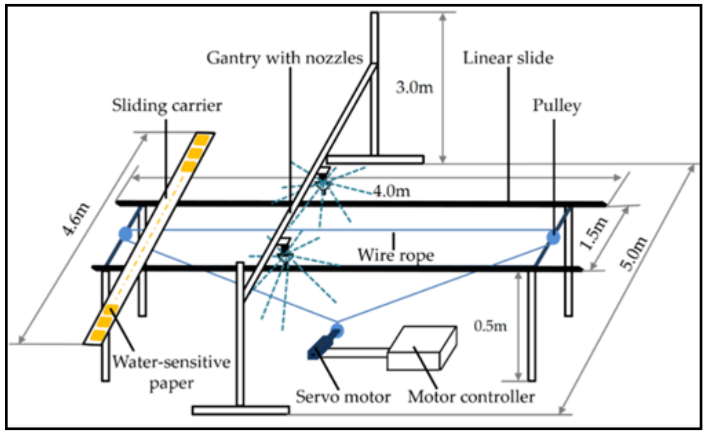

Figure 5. Schematic of spraying platform by *Wang, 2022*.

The test is now conducted by spraying 2 WSP instead of 6. The WSP measures 52 mm x 76 mm. They are placed 300 mm away from the center of the spray. This allows for a smaller swathe, increasing stability during motion; however, the height is still not constant. The development of a test rig that keeps the height constant during a constant speed would increase the precision of the method of test.

There are test benches that utilize a gantry system for spray droplet sizing. A low-cost test bench was developed that prioritized carrying the nozzle at a set speed along a 3 m rail shown in **Figure 3**. It was powered by a DC motor. The droplets fell into mineral oil filled petri dishes. The coefficient of variation of the VMD was between 1.9% to 8.6% (Longo et al., 2020).

A spray-painting robot was developed using a gantry system as shown in **Figure 4**. It used an aluminum V-slot railing and stepper motors. The spraying robot was designed for painting. The coefficient of variation was found to be low at 32.65% (Jasim et al., 2023).

Another system was designed for analyzing the influence of parameters of unmanned aerial vehicles (UAV) application spraying systems. It utilized gantry rails and was powered by servo motors as shown in **Figure 5**. It was controlled using a motor controller and software. It also utilized water sensitive papers The standard deviation of the positioning was 0.4mm (Wang et al., 2022).

Arduino microcontrollers are a good option for motion control systems The open-source nature of the platform allows for versatility when it comes to designing software control. They are widely used in systems with stepper motors, DC servo motors, and robotics. Studies with linear positioning drives typically utilize Proportional–Integral–Derivative (PID) control and Pulse Width Modulation (PWM) for motor control (Abreu et al., 2020). These systems are built on a closed-loop control that integrates signals obtained from sensors or encoders, promoting accuracy and stability (Ali et al., 2017). The microcontroller is interfaced with development tools such as Arduino IDE, which is a free software. There are libraries which can be used to simplify design.

The main objective of this study was to develop and evaluate a test rig for determining the volumetric median diameter of the spray droplets of agricultural sprayers. It also aimed to formulate a protocol for using and maintaining the test rig.

The study employed a knapsack sprayer for testing. The experimental design was based on pre-existing data from the Agricultural Machinery Testing and Evaluation Centre, College of Engineering and Agro-Industrial Technology, University of the Philippines Los Baños. Other agricultural sprayers may be tested with the developed test rig. However, the design primarily focused on nozzles used by knapsack sprayers. Nozzles with multiple heads may potentially be incompatible with the test rig. Operation relies on a stable hold on the nozzle and grip of the knapsack sprayer. The length of the hose is a limiting factor, as the carriage has a set distance that must be traversed. It was also constrained by the available materials and equipment. The test report of the sprayer is also under a non-disclosure agreement.

MATERIALS AND METHODS

Design of the Test Rig Frame

The test rig was intended to emulate the method of test in the Philippine National Standard. The spraying operation was split into three phases: pre-spray, spray and post spray phases as indicated in **Figure 6**.

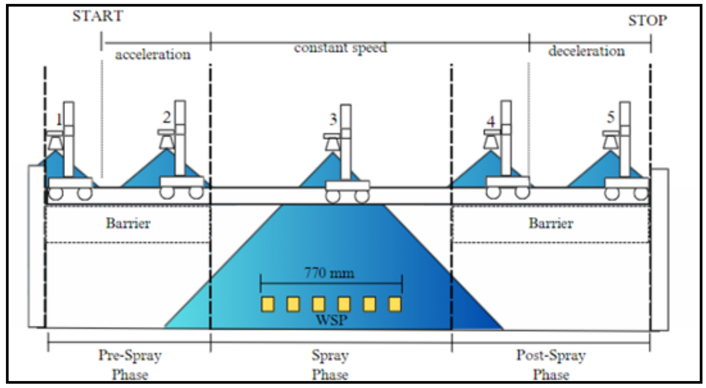

Figure 6. Spray operation phases.

The spray phases determined the dimensions of the test rig. The nozzle tip is approximately 1000 mm above the WSP. The most common spray angles of nozzles are 65º, 80º, and 110º (Miller & Bellinder, 2001). The width accommodates the spray width of a nozzle with a 110º spray angle. The nozzle was positioned 40 mm above the spray barriers. The theoretical spray width at the top surface of the spray barriers was calculated to be 114 mm using **Equation 1**.

$$b = 2 * a * \tan(\frac{\theta}{2}) \qquad \textbf{\textit{Equation 1}}$$

Where:

b theoretical spray width (mm)

a vertical distance between nozzle and spray barrier (mm)

Θ angle of spray (º)

The frame was open to prevent splattering. Its length was based on the available V-slot aluminum extrusion. Each railing measures 1800mm in length. The pre-spray phase was shorter due to the open end, which was 400 mm long. The spray phase was the longest at 900 mm, while the post-spray phase spanned 500 mm to keep the nozzle within the frame after spraying. The frame measured 1005 mm in height, 600 mm in width, and 1900 mm in length. Including the stands for power components, the total length was 2400 mm. The WSP sheets were placed on a height-adjustable platform, with the platform arms being 3D-printed. The platform was clamped in the Spray Phase Area.

Design of the Spray Barriers

The spray barrier is shown in **Figure 7**. It prevented the spray droplets during the acceleration and stopping phases of the operation. Open-cell foam was used to prevent the droplets from deflecting against the plastic surface. The collision between the foam and the droplets disperses the kinetic energy of the droplets. (de Carvalho et al., 2023). Melamine foam was placed under the open-cell foam to absorb any droplets that passed through. (Wang D., 2012). The spray barriers are made of Polyethylene plastic. This prevented any deflection or adhesion of the droplets, preventing undesired markings on the WSP (Picuno et al., 2024).

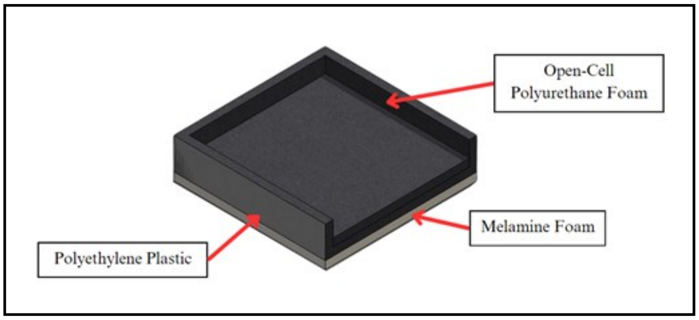

Figure 7. Spray barrier.

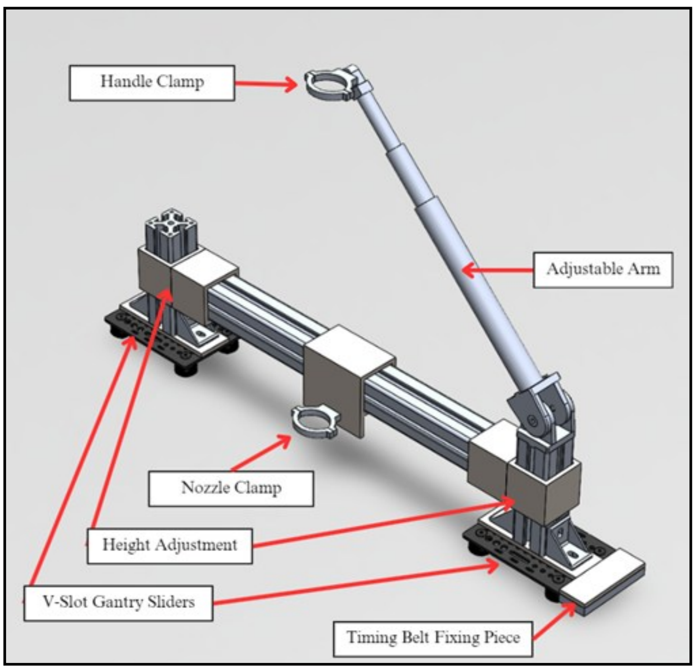

Figure 8. Carriage components.

The interior walls of the spray barriers were padded with open-cell polyurethane foam. This effectively drew the caught spray droplets to the interior base. The base was padded with melamine foam to collect the fluid. The spray barriers were bolted in the Pre-Spray and Post Spray areas.

Design of the Carriage

The design of the carriage focused on keeping the handheld components of the knapsack sprayer securely in place. The components are shown in **Figure 8**.

An adjustable arm was made from a telescoping rod affixed fixed to a hinge. The nozzle is in a fixed position during the operation. The nozzle clamp was mounted to a slider. It was bolted to the center of the carriage using T-nuts. The nozzle clamp was adjustable to accommodate different nozzle types and their dimensions. The position of the nozzle clamp is also adjustable to account for any errors. The carriage featured a removable arm for sprayer components that required stability. The angle of bend of the nozzle relative to the lance was addressed by mounting the arm on a hinge. The timing belt fixing piece was mounted to one end of the carriage. It had an opening for the open ends of the timing belt.

The materials used for the gantry sliders, hinge, adjustable arm, nozzle clamp, and timing belt fixing piece are aluminum 6061-T1. The material of the v-slot wheels of the gantry sliders is polyoxymethylene (POM), Delrin® brand. The handle clamp was made from plastic. The height adjustment sliders were custom-made from Stainless Steel 316.

Timing Belt and Motor Selection

The test rig can be considered as a linear positioner in a horizontal configuration. The selection of the belt was calculated using **Equation 2** (Gates Mectrol, 2006). The effective tension in the belt determines the belt profile.

$$T_e = F_a + F_f \qquad \text{Equation 2}$$

Where:

T_e effective tension in belt (N)

F_a force required to accelerate the carriage (N)

F_f frictional force between v-slot wheels and the railing (N)

The values F_a of F_f and were calculated using **Equations 3 and 4**. The carriage weighed 4kg after fabrication. The coefficient of friction between the POM wheel and aluminum was found to be 0.15 (Jozwik, 2020).

$$F_a = m_c * a \qquad \textit{Equation 3}$$

Where:

F_a is the force required to accelerate the carriage (N)

m_c is the mass of the carriage (kg)

a is the required acceleration of carriage (m/s^2)

$$F_f = \mu_k * W_c \qquad \textit{Equation 4}$$

Where:

F_f is the frictional force between the v-slot wheels and the railing (N)

μ_k is the friction between the POM wheel and aluminum

W_c is the mass of the carriage (kg)

The calculated tension was 10.52 N. The selected belt profile is HTD5M. The available belt width was 15mm. The calculated tension falls within the recommended value, as shown in **Figure 9**. The total length of the open-ended belt was 5.

The selected motor was a Wantai Geared Stepper Motor, NEMA 34, with a holding torque capacity of 175 kg-cm. The motor was mounted on the frame itself. This allowed for a direct transmission to the driver pulley. Due to a lack of data from the manufacturer and distributor, the maximum running torque of the motor was experimentally determined.

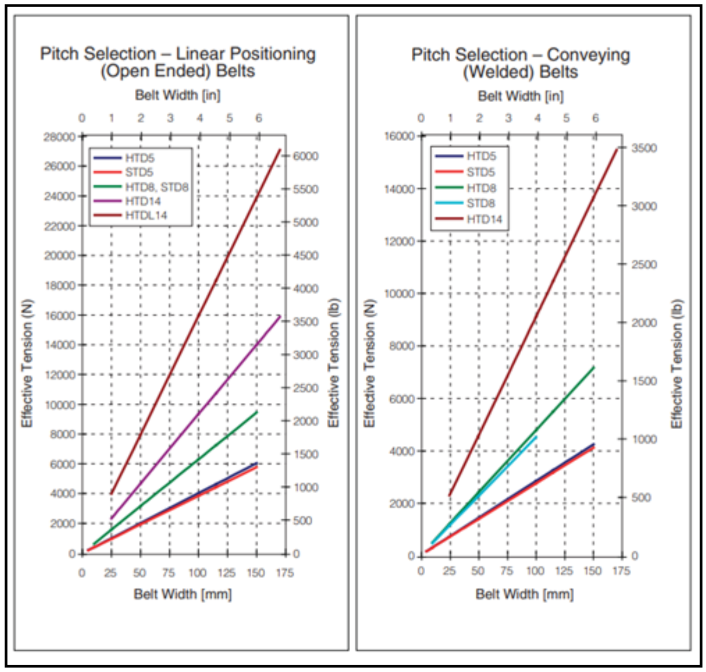

Figure 9. Pitch selection for linear positioning *from Gates Mectrol, 2006*.

Starting from 770 mm/s, the speed was changed the moment the motor would stall. After each stall, the power supply was turned off until the stepper cooled down. The criteria for a reliable speed setting should show no signs of heating or stalling even after 10 trials. The calculated lengths covered during acceleration and deceleration were 181 mm and 443 mm, respectively.

The original times for acceleration and deceleration at a target speed of 770 mm/s were 0.66 s and 1.15 s, respectively. To prevent spray droplets from contacting the WSP while accelerating and decelerating, the constant speed time was increased by incorporating half of the spray width into the constant speed length. The time for constant speed was set to 1.32 s. The observed spray time should be approximately 1.16 seconds. With 99% efficiency of timing belts, the theoretical time to traverse the spray length should be approximately 1.18 seconds.

Circuit and Software Control Design

The microcontroller used was an Arduino UNO R3. The motor was connected to a DQ860MA Microstep Driver. It is responsible for conveying the electrical signals to the stepper motor from the microcontroller. The pulses per revolution were set to 800, therefore, the microstepping factor is 4. The power supply was set to 24V and 8.3A.

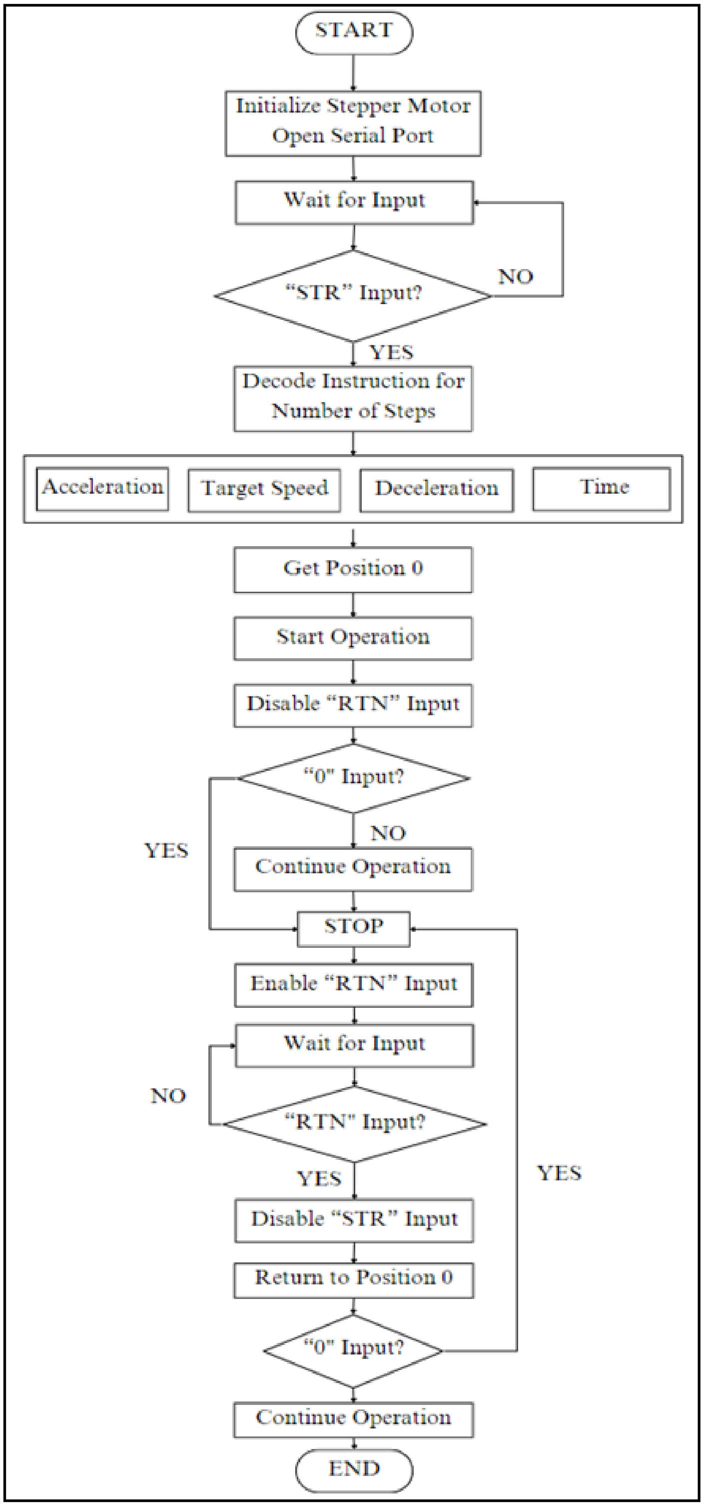

Figure 10. Software control chart.

The software control was developed using the Arduino IDE (v. 2.3.3) and utilized the FastAccelstepper library (ver. 0.30.15) for coding. This library is designed for programming stepper motors that operate at high speeds and accelerations. It simplifies the input of acceleration, deceleration, target speed, and target positions, while also tracking the distance traveled (Kiemes, 2020).

The target position was a crucial input, as the operation involves the carriage returning to its starting point. The commands would be input into the serial monitor. The "STR" command would start the operation. The "RTN" command returned the carriage to the start point. "0" would trigger the emergency stop. To prevent errors due to conflicting command inputs, the software control would ignore "RTN" during the spraying operation and ignore "STR" during the operation. The software control flowchart is shown in **Figure 10**.

Evaluation Method

The primary considerations for evaluating the performance of the test rig were spray time, and the VMDe spray time was measured using a stopwatch. The time was measured between the end of the Pre-Spray length and the end of the Spray Phase. The WSPs were cut into six pieces, each measuring 20 mm by 30 mm. The WSP was cut beforehand in a closed, air-conditioned room to prevent the hue from changing. Three trials were conducted for every pressure and nozzle setting. WSP cards measuring 52 mm x 76 mm were also prepared. These were for conducting the method of test developed by UPLB-AMTEC. This was the same method of test used to obtain data for the official test report of the sprayer. The test report and the experimental results were compared. All WSPs were stored in resealable bags immediately after every trial. The three pressure settings for the knapsack sprayer were 275 kPa, 358 kPa, and 441 kPa. The two nozzles used were a Single Head Single Orifice (SHSO) and a Single Head 4-Orifice Nozzle (SH4O).

Spray time and VMD were measured for every trial. The testing of the test rig only utilized nozzles from a knapsack sprayer, with pre-existing readings from the available AMTEC test report. No other types of agricultural sprayers were tested.

During testing, the operator wore the knapsack sprayer, and the researcher controlled the test rig from the computer. The WSP was placed on the WSP Platform prior to every test. The platform was wiped clean before and after every test. The height between the WSP and the nozzle was taken after the component had been switched.

The electronic components were covered to prevent damage. The operator also took the readings of Spray Time using a stopwatch. The spray times were recorded immediately after every test. The melamine foam in the spray barriers was wrung after every trial. The knapsack sprayer had a pressure gauge installed between the hose and the handle. The pressure reading on the gauge was stable before the cut-off valve was opened and locked. The output of the electric-motor-driven knapsack sprayer was then adjusted until the pressure reading indicated that the target pressure had been reached.

The "STR" command was then input into the software control to start the carriage motion. Once the carriage reached the end of the rails, the operator turned off the cut-off valve. The WSP was removed from the WSP Platform. "RTN" was then input into the software control to return the carriage to the starting point. The power supply should be turned off first while waiting for the WSP to dry. This allowed the motor to rest. The WSP platform was wiped, and the next set of WSPs were prepared for the next trial.

The images were taken in a bright room with a 12MP, 3000x4000-pixel, 69 mm, ISO 40, f/2.4 camera. The measurement of the VMD was conducted using ImageJ. The images were converted to 8-bit greyscale. The threshold setting was adjusted to enhance droplet detection. A scale was set in pixels per micron. ImageJ was used to calculate the droplet diameters and VMD. The outlines detected by ImageJ were displayed to validate the analysis. The averages of the VMD for each WSP in each trial were recorded.

The average VMD from the WSP cards was employed to compare the precision of each trial. The precision of the VMD was measured by analyzing the coefficient of variation (CV), a method similar to that used by Longo et al. (2020) in their test bench study. The CV was calculated using **Equation 5**.

$$CV = \frac{standard\ deviation}{\text{mean}}\ x\ 100$$ ***Equation 5***

RESULTS AND DISCUSSION

Fabricated Test Rig

The fabricated test rig is illustrated in **Figures 11 and 12**. The frame was fabricated first. This ensured that the dimensions of the mount are aligned with the placement of the railings. The railings were then installed onto the frame with only one end secured with the rail guard. The carriage was then fabricated and mounted. The alignment was verified by running the carriage over the 2080 V-slot rails. The other rail guard was bolted down. The motor, flexible coupling, and pulleys were then mounted. The timing belt was mounted and tensioned. The open ends were pulled through the timing belt fixing piece. The pulleys were aligned and locked into place. The railings were also lubricated to reduce friction.

The test rig was calibrated afterwards. The target speed, acceleration, and time were adjusted until the carriage completed the track. The electronic components were positioned a safe distance away. The handheld components of the sprayer were subsequently placed into the carriage, as shown in **Figure 13**.

Performance Evaluation

The test rig was designed to move the carriage at a constant speed over the spray area. The time taken to pass all the WSPs is approximately 1 second. The length to cover the WSPs is 770mm. This information is based on section 7.6.4.e of PNS/BAFS 332:2022. The distance between the nozzle and the WSP was 1000 mm as per section 7.6.4.d of PNS/BAFS 332:2022.

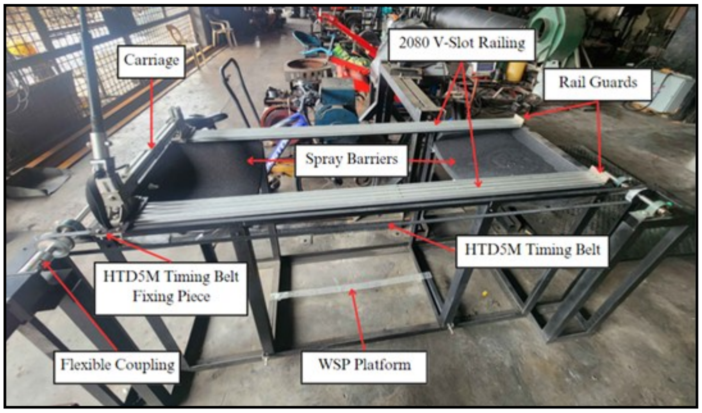

Figure 11. Fully fabricated test rig.

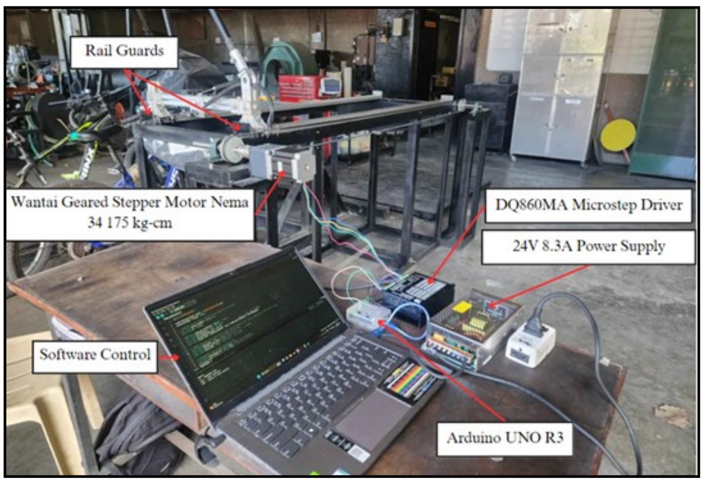

Figure 12. Test rig with electronic components.

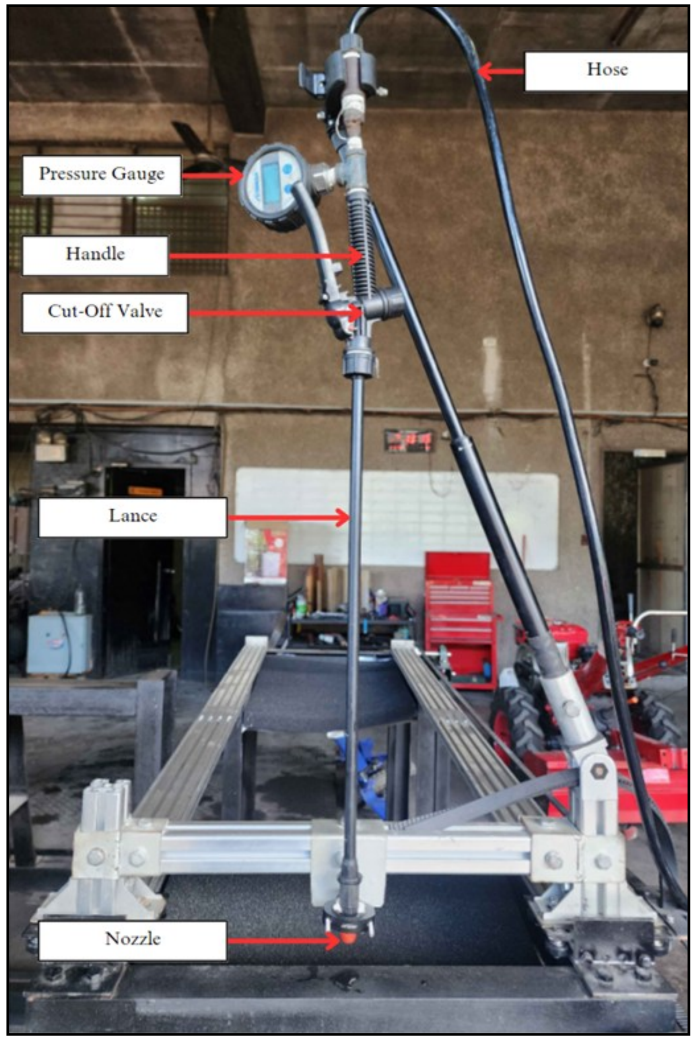

Figure 13. Carriage with handheld components.

Table 1. Maximum speed setting trial.

Trial	670 mm/s		660 mm/s		650 mm/s	
	Time	Remark	Time	Remark	Time	Remark
1	1.39	none	1.39	none	1.4	none
2	1.39	none	1.39	none	1.39	none
3	1.38	Heat	1.38	none	1.39	none
4	1.37	Heat	1.37	none	1.38	none
5	1.40	Heat	1.40	none	1.41	none
6	1.42	Heat	1.42	Heat	1.40	none
7	1.41	Heat	1.38	Heat	1.40	none
8	1.41	Heat	1.41	Heat	1.40	none
9	1.41	Heat	1.41	Heat	1.41	none
10	1.43	Stall	1.43	Heat	1.39	none

The test rig was run multiple times without any handheld components mounted. The acceleration and deceleration settings were retained. The target speed had to be changed due to insufficient data regarding the motor. The initial target speed setting was at 770 mm/s; however, target speed settings from 770 mm/s to 680 mm/s stalled during operation.

The target speed setting that did not show heating over 10 trials was 650 mm/s, as indicated in **Table 1**. The average time to cover the Spray Phase length was 1.397 s. This indicates that all WSPs are sprayed in approximately 1.18 seconds. The standard deviation was 0.009 seconds. The coefficient of variation was found to be 0.679%.

It has a calculated constant speed time of 2.00s. After calibration, the setting for constant speed was 2.3s to complete the track. The acceleration and deceleration settings were not changed to prevent the speed from changing during the spray length. The lengths for acceleration and deceleration at the new speed were calculated to be 181 mm and 314 mm, respectively. The maximum acceleration length was 255mm, and the deceleration length was 443mm. The new lengths were less than the maximum values. This indicates that the speed remains constant during the spray length.

Spray Time Precision

The coefficient of variation of the test rig for every knapsack sprayer configuration is shown in **Table 2**. The SHSO (Configuration A) and SH4O (Configuration B) nozzles changed the position of the adjustable arm. The shift in position may cause an imbalance in the carriage, which affects spray time. The spray times of both configurations were compared. The coefficient of variation was consistently low. The mean spray times were consistently around 1.4 s for Configuration A. Configuration B had a slightly higher mean spray time. However, this could be a result of human error. The highest CV was 1.09%. This indicates that the test rig remains precise across different configurations.

Table 2. Precision of test rig vs. nozzle type and pressure.

TRIAL Pressure (kPa)	NOZZLE TYPE			
	SHSO		SH4O	
	Mean Spray Time (s)	CV (%)	Mean Spray Time (s)	CV (%)
1 (275)	1.41	1.09	1.42	0.81
2 (358)	1.397	0.41	1.43	0.40
3 (441)	1.41	0.71	1.42	1.08

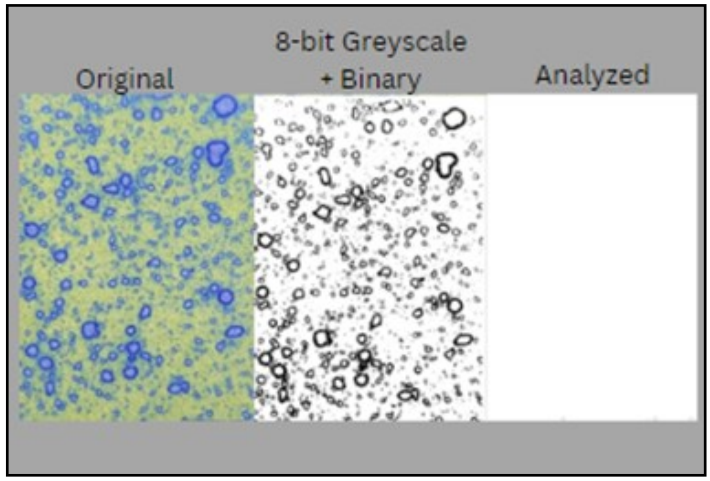

Figure 14. Trial of imageJ analysis of unreadable WSP (SHSO).

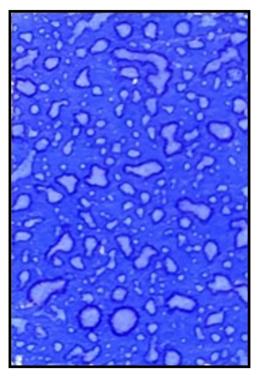

Figure 15. Unreadable WSP due to nozzle leakage.

VMD Precision

The WSP cards were removed from the WSP platform after every trial. They were dried between 1 -5 minutes or until dried as per PNS/BAFS 332:2022. The WSP cards were then placed into resealable bags to prevent exposure to moisture.

Due to the long wait time before storage, the WSP cards became unreadable by ImageJ. A sample of unreadable WSP is presented in **Figure 14**.

The SH4O nozzle exhibited leakage, as indicated in the test report. This resulted in ImageJ being unable to measure any droplets. The markings on the WSP are where the water pooled on the surface of the WSP card. This also caused the WSP card to warp. An example of this is shown in **Figure 15**.

The analysis of spray droplet sizes was performed using the current test method of AMTEC, CEAT-UPLB instead. The same testing method was used in the test report. Using this approach enables a better comparison between the VMD result from the test rig and the report data. The SHSO nozzle was used. Due to regulatory constraints, the SH4O nozzle could not be repaired. Repairing it may potentially violate the non-disclosure agreement. The pressure was set to maximum at 441 kPa. Two (2) WSP cards were used instead of 6 per trial. The dimensions of the cards were 52 mm x 76 mm. They were each placed at the sides of the center of the spray, with intervals of 300 mm. The spray was still delivered at 1000 mm above the WSP at the same speed setting. The cards were scanned right away after the spray. The brand of the WSP is the same brand used by the test engineer during the testing of the knapsack sprayer. The ambient conditions during this test were 29°C and 90% relative humidity (RH).

There was some rain and minimal winds during the testing. The settings used in ImageJ were dependent on the pixel dimensions of the cropped image. The scales were set by basing them on the physical dimensions of the card. No HSB thresholding was done. The thresholding was done by visually determining which of the highlighted marks are considered drops. The pixel limit during analysis of droplet areas was determined by estimating which of the included marks were incomplete drops.

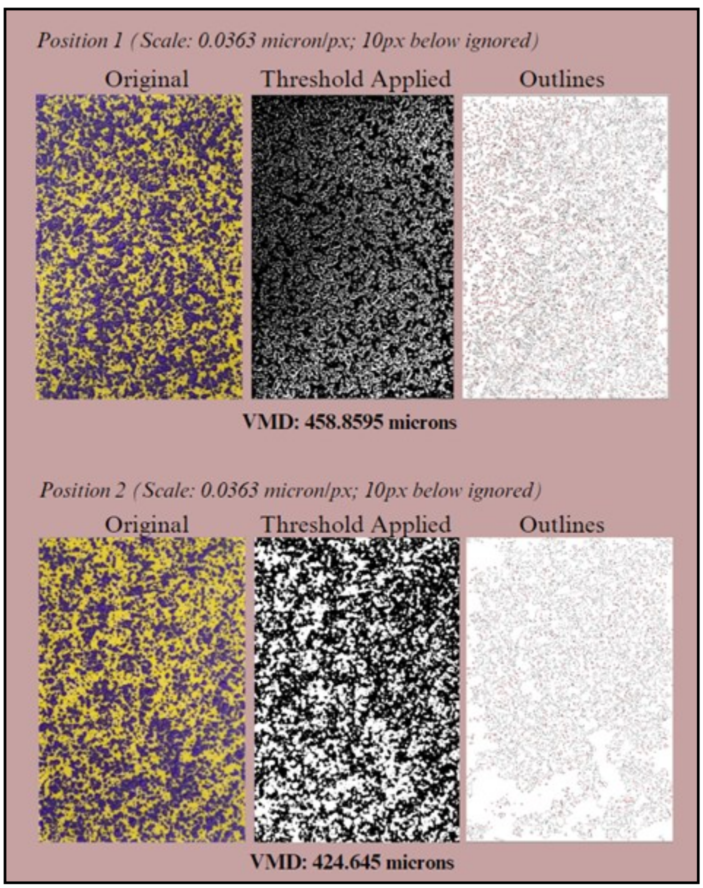

Figure 16. Trial 1 analysis of WSP.

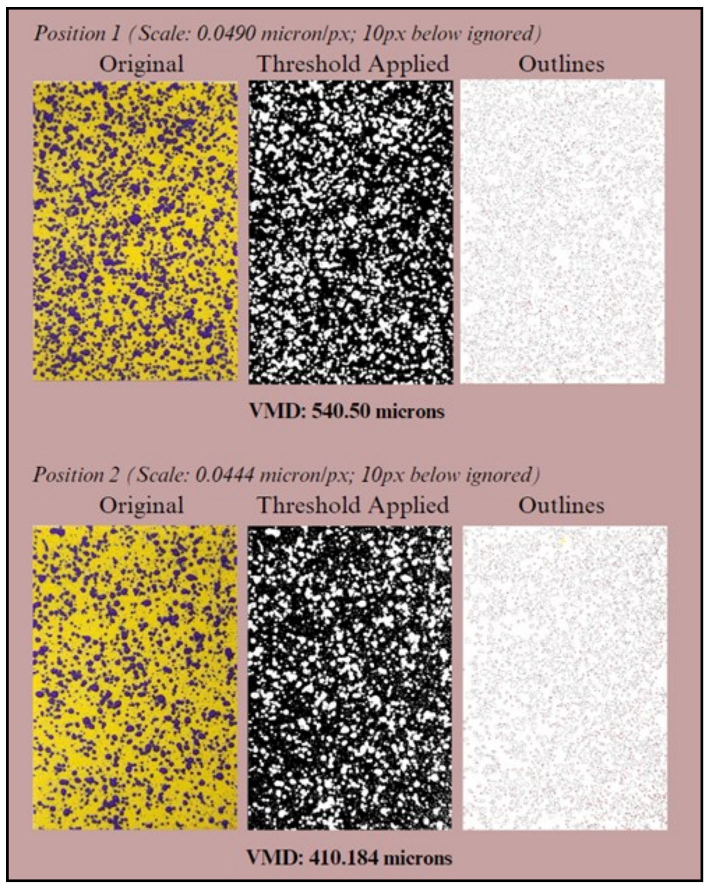

Figure 17. Trial 2 analysis of WSP.

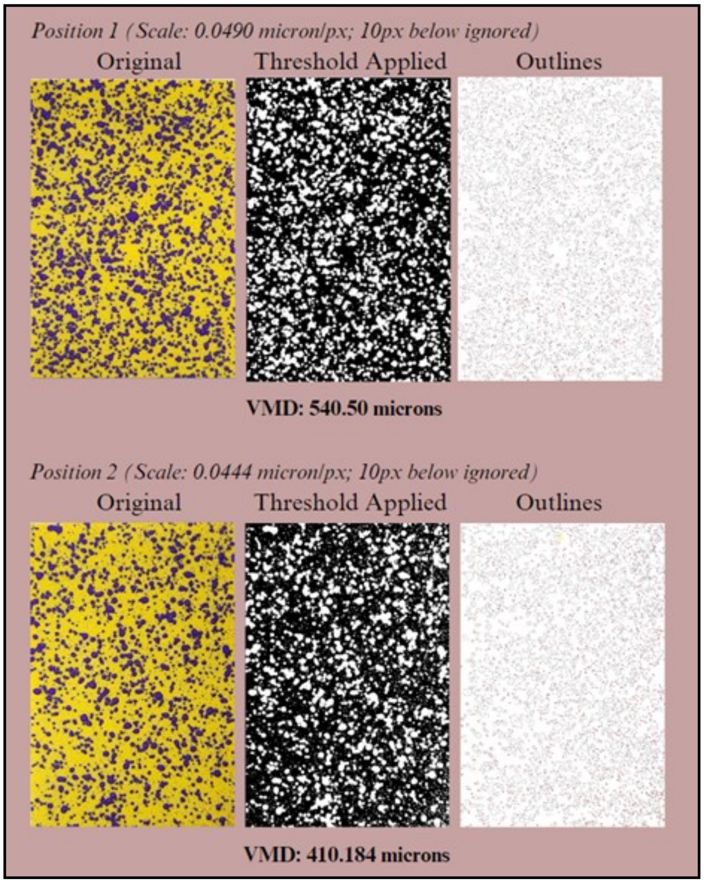

Figure 18. Trial 3 analysis of WSP.

Table 3. Classification of VMD averages.

Trial	VMD (MICRONS)			Classification
	POS 1	POS 2	AVG	
1	458.86	424.65	441.75	VERY COARSE
2	540.50	410.18	475.34	VERY COARSE
3	501.96	492.16	497.06	VERY COARSE
Test Report	502	480	491	VERY COARSE

The edges were ignored, and the outlines were generated post-analysis. The results of the area per droplet were used to calculate the diameters of the individual droplets. The classification of the spray droplet diameter was performed by calculating the average of the VMD values from the two cards. The classification of each trial was compared with the test report. **Figures 16, 17, and 18** display the results of the analysis performed using ImageJ.

The results of this test are presented in **Table 3**. The trials all yielded a classification of “VERY COARSE”. This corresponds to the droplet size classification of the knapsack sprayer in the test report, which was 491 microns. The first position yielded a higher VMD compared to the second position, which was consistent across all trials.

The CV of the trials also shows a low value of 5.91%. This indicates that the test rig is capable of precisely determining the VMD of the spray droplets.

CONCLUSION

The motor operated at a maximum speed of 650 mm/s, resulting in an average spray length time of 1.397 s and an average spray time over all WSPs of 1.18 s. The highest recorded spray length time was 1.43 s (Configuration B, Trial 2), and the lowest was 1.397 s (Configuration A, Trial 2). The test rig demonstrated high precision with spray times, with a coefficient of variation (CV) of less than 1.09%.

The experimental method followed the same procedure used in the original test report, rather than the PNS/BAFS 332:2022 standard. VMD testing also showed high consistency, with a CV of 5.91%, and all trials were classified as "VERY COARSE," matching the test report. These results confirm the test rig's capability to accurately and consistently measure spray droplet size, even with the modifications in the experiment.

RECOMMENDATIONS

Implementation of sensors for detecting the actual speed of carriage would increase the precision of the evaluation. Alternatively, a design where the WSP Platform moves instead of the nozzle should also be explored. This allows for a lower motor capacity requirement. Additional nozzle types and more types of sprayers should also be evaluated on the rig. Adding a compartment for the sprayer tank would also eliminate the need for an operator.

The utilization of a motor with known Torque-RPM curves would also improve the linear positioning drive. This allows for an increased range of spray times that can be tested. Different heights for the WSP should also be studied. The different heights may yield more consistent VMD readings. The spray barriers also sagged during the operation. A more durable material than Polyethylene plastic would be appropriate. Wind may potentially affect the readings of the VMD. A barrier around the whole sprayer would reduce this. A cover for the electronic components would also improve the safety of the test rig.

ACKNOWLEDGEMENT

The authors would like to acknowledge the Agricultural Machinery Testing and Evaluation Center (AMTEC), College of Engineering and Agro-Industrial Technology (CEAT), University of the Philippine Los Baños (UPLB) for the technical and logistic support, and the Agribiosystems Machinery and Power Engineering Division (AMPED), Institute of Agricultural and Biosystems Engineering (IABE), CEAT, UPLB, for the use of equipment and facilities.

LITERATURE CITED

ABREU, J., SILVA, A., SOUZA, J., & SENA, A. (2020). Sistema Embarcado Para O Controle De Posição De Um Robô Paralelo Tipo Delta Linear De Baixo Custo. *Perspectivas das Engenharias na Sociedade 5.0: Educação, Ciência, Tecnologia e Amor.* Retrieved from https://www.researchgate.net/publication/348902960_SISTEMA_EMBARCADO_PARA_O_CONTROLE_DE_POSICAO_DE_UM_ROBO_PARALELO_TIPO_DELTA_LINEAR_DE_BAIXO_CUSTO.

AL HEIDARY, M., DOUZALS, J., SINFORT, C., & ARIANE, V. (2014). Influence of spray characteristics on potential spray drift of field crop sprayers: A literature review. *Crop Protection*, 120-130. Retrieved from https://www.researchgate.net/publication/263353170_Influence_of_spray_characteristics_on_potential_spray_drift_of_field_crop_sprayers_A_literature_review/citation/download.

ALI, A., AHMED, A., ALMAHDI, H., TAHA, O., & NASERALDEEN, A. (2017). Design and Implementation of Ball and Beam System Using PID Controller. Retrieved from https://www.researchgate.net/publication/317079231_Design_and_Implementation_of_Ball_and_Beam_System_Using_PID_Controller.

ANJUM, M., CHEEMA, M., HUSSAIN, F., & WU, R. (2023). *Precision Agriculture.* Academic Press. doi:https://doi.org/10.1016/B978-0-443-18953-1.00007-6.

ASABE STANDARDS (2009). S572.1: Spray Nozzle Classification by Droplet Spectra. American Society of Agricultural and Biological Engineers, St. Joseph, MI., 4 pp.

BHUSE PK, V. R. (2014). Ergonomic Evaluation of Knapsack Sprayer used in Agricultural Application. *International Journal of Scientific and Engineering Research*, 903-904.

BUREAU OF AGRICULTURE AND FISHERIES STANDARDS (BAFS) . (2022). Knapsack Sprayer – Methods of Test. In *Philippine National Standards (PNS)* (p. 6).

DE CARVALHO, T., HARGREAVES, D., & MORVAN, H. (2023). Modelling of Droplet Capture in an Open-Cell Metal Foam at the Pore and Macroscopic Scales. *Transp Porous Med*. Retrieved from https://link.springer.com/article/10.1007/s11242-023-01918-4#citeas.

GATES MECTROL, INC. (2006). *Belt Sizing Guide.* Retrieved from GATES MECTROL: https://assets.gates.com/content/dam/gates/home/knowledge-center/mectrol/design-manuals/BeltSizingGuide.pdf.

JASIM, F., ALI, M., & HAMAD, A. (2022). Design and Analysis of a Spraying Robot. *Al-Khwarizmi Engineering Journa*, 1-14.

JOZWIK, J. D. (2020). Analysis and Comparative Assessment of Basic Tribological Properties of Selected Polymer Composites. *Materials*, 75.

KIEMES, J. (2020). *gin66/FastAccelStepper.* Retrieved from GitHub: https://github.com/gin66/FastAccelStepper?tab=MIT-1-ov-file.

LONGO, D., MANETTO, G., PAPA, R., & CERRUTO, E. (2020). Design and Construction of a Low-Cost Test Bench for Testing Agricultural Spray Nozzles. *Applied Sciences*. Retrieved from https://www.mdpi.com/2076-3417/10/15/5221.

LU, J. (2022). Assessment of Pesticide-Related Pollution and Occupational. *Acta Med Philipp [Internet]*, 30-36. doi:https://actamedicaphilippina.upm.edu.ph/index.php/acta/article/view/3868.

MILLER, A., & BELLINDER, R. (2001). *Herbicide Application Using a Knapsack Sprayer.* Retrieved from KnowledgeBank: http://www.knowledgebank.irri.org/csisa/images/FactsheetsAndReferences/references/sprayerenglish.pdf.

PICUNO, C., GODOSI, Z., SANTAGATA, G., & PICUNO, P. (2024). Degradation of Low-Density Polyethylene Greenhouse Film Aged in Contact with Agrochemicals. *Applied Sciences*, 10809.

WANG, D. (2012). Preparation and Property Analysis of Melamine Formaldehyde Foam. *Advances in Materials Physics and Chemistry*, 63-67. ■